

1 **LEVERAGING CHORIONIC VILLUS BIOPSIES FOR THE DERIVATION OF PATIENT-SPECIFIC**  
2 **TROPHOBLAST STEM CELLS**

3  
4 **Kaela M. Varberg<sup>1,†,\*</sup>, Ayelen Moreno-Irusta<sup>1,†</sup>, Allynson Novoa<sup>2</sup>, Boryana Koseva<sup>3,4</sup>, Brynne**  
5 **Musser<sup>1</sup>, Joseph M. Varberg<sup>5</sup>, Jeremy P. Goering<sup>6</sup>, Irfan Saadi<sup>8</sup>, Hiroaki Okae<sup>7</sup>, Takahiro Arima<sup>7</sup>,**  
6 **John Williams III<sup>8,9</sup>, Elin Grundberg<sup>1,3,4</sup>, Margareta D. Pisarska<sup>2,8,9,10\*</sup>, and Michael J. Soares<sup>1,4,11,\*</sup>**  
7

8 <sup>1</sup>Institute for Reproductive and Developmental Sciences, Department of Pathology & Laboratory  
9 Medicine, University of Kansas Medical Center, Kansas City, KS 66160

10  
11 <sup>2</sup>Division of Reproductive Endocrinology and Infertility, Department of Obstetrics and Gynecology,  
12 Cedars-Sinai Medical Center, Los Angeles, CA

13  
14 <sup>3</sup>Genomic Medicine Center, Children's Mercy Research Institute, Children's Mercy Kansas City, Kansas  
15 City, MO

16  
17 <sup>4</sup>Center for Perinatal Research, Children's Mercy Research Institute, Children's Mercy, Kansas City, MO  
18 64108

19  
20 <sup>5</sup>Stowers Institute for Medical Research, Kansas City, MO, 64110

21  
22 <sup>6</sup>Department of Cell Biology and Physiology, University of Kansas Medical Center, Kansas City, KS  
23 66160

24  
25 <sup>7</sup>Department of Informative Genetics, Environment and Genome Research Center, Tohoku University  
26 Graduate School of Medicine, Sendai 980-8575, Japan

27  
28 <sup>8</sup>Department of Obstetrics and Gynecology, Cedars-Sinai Medical Center, Los Angeles, CA

29  
30 <sup>9</sup>David Geffen School of Medicine, University of California, Los Angeles, CA

31  
32 <sup>10</sup>Department of Biomedical Sciences, Cedars-Sinai Medical Center, Los Angeles, CA

33  
34 <sup>11</sup>Department of Obstetrics and Gynecology, University of Kansas Medical Center, Kansas City, KS  
35 66160

36  
37 **Running title:** Chorionic villus-derived human TS cells

38  
39 <sup>†</sup>Authors contributed equally to the manuscript.

40  
41 **\*Correspondence:** Kaela M. Varberg, [kvarberg@kumc.edu](mailto:kvarberg@kumc.edu); Margareta D. Pisarska,  
42 [margareta.pisarska@cshs.org](mailto:margareta.pisarska@cshs.org); Michael J. Soares, [msoares@kumc.edu](mailto:msoares@kumc.edu)  
43

44 **Keywords:** trophoblast stem cells, chorionic villus sampling, placental development

## 45 **Abstract**

46 Human trophoblast stem (**TS**) cells are an informative in vitro model for the generation and testing  
47 of biologically meaningful hypotheses. The goal of this project was to derive patient-specific TS cell lines  
48 from clinically available chorionic villus sampling (**CVS**) biopsies. Cell outgrowths were captured from  
49 human CVS tissue specimens cultured in modified human TS cell medium. Cell colonies emerged early  
50 during the culture and cell lines were established and passaged for several generations. Karyotypes of  
51 the newly established CVS-derived trophoblast stem (**TS<sup>CV</sup>**) cell lines were determined and compared to  
52 initial genetic diagnoses from freshly isolated chorionic villi. Phenotypes of **TS<sup>CV</sup>** cells in the stem state  
53 and following differentiation were compared to cytotrophoblast-derived TS (**TS<sup>CT</sup>**) cells. **TS<sup>CV</sup>** and **TS<sup>CT</sup>**  
54 cells uniformly exhibited similarities in the stem state and following differentiation into syncytiotrophoblast.  
55 These shared features included morphology and gene expression. **TS<sup>CV</sup>** cell differentiation into  
56 extravillous trophoblast cells exhibited cell line dependent phenotypes. CVS tissue specimens provide a  
57 valuable source for TS cell derivation. They expand the genetic diversity of available TS cells and are  
58 associated with defined clinical outcomes. **TS<sup>CV</sup>** cell lines provide a new set of experimental tools for  
59 investigating trophoblast cell lineage development.

60

## 61 **Introduction**

62 Chorionic villus sampling (**CVS**) represents a standard, prenatal care procedure that is performed  
63 between 10-14 weeks of gestation (Stranc et al., 1997). Sampling involves the removal of a small amount  
64 of chorionic villus tissue, for the purpose of genetic testing. Common indications for retrieving chorionic  
65 villus tissue include advanced maternal age, history of infertility, family history, including another child  
66 with genetic anomalies, or an abnormal noninvasive prenatal test result (Pisarska et al., 2016; Stranc et  
67 al., 1997). In addition to their use in genetic diagnosis, first trimester chorionic villus tissue has become a  
68 robust platform for investigation of placental pathobiology (Flowers et al., 2021; Gonzalez et al., 2021;  
69 Pisarska et al., 2016). Chorionic villi are comprised of several cell types including trophoblast cells,  
70 mesenchymal cells, macrophages, and cells comprising fetal blood vessels (Aplin and Jones, 2021; Sun  
71 et al., 2020). The villus trophoblast cell compartment includes two primary populations, i) cytotrophoblast  
72 and ii) terminally differentiated syncytiotrophoblast (**STB**; Aplin and Jones, 2021). Cytotrophoblast have

73 the capacity to self-renew, and to differentiate into either extravillous trophoblast (**EVT**) cell or STB  
74 lineages (Knöfler et al., 2019; Soares et al., 2018). Regulatory mechanisms underlying human  
75 cytotrophoblast self-renewal and differentiation have largely remained elusive.

76

77 In 2018, conditions for capturing and maintaining human trophoblast stem (**TS**) cells in vitro were  
78 first described (Okoe et al., 2018). Human TS cells have the capacity for self-renewal and differentiation  
79 into EVT cells or STB. This in vitro model system has led to the generation of new insights into  
80 mechanisms regulating human trophoblast cell development (Bhattacharya et al., 2020; Hornbachner et  
81 al., 2021; Ishiuchi et al., 2019; Jaju Bhattad et al., 2020; Muto et al., 2021; Perez-Garcia et al., 2021;  
82 Ruane et al., 2022; Saha et al., 2020; Shahbazi et al., 2020; Shannon et al., 2022; Sheridan et al., 2021;  
83 Takahashi et al., 2019; Varberg et al., 2021). Initial human TS cell lines were derived from blastocysts, or  
84 first trimester placental tissue obtained from pregnancy terminations. Establishment of culture conditions  
85 for human TS cells led to the derivation of TS cells from pluripotent stem cells (Castel et al., 2020;  
86 Cinkornpumin et al., 2020; Dong et al., 2020; Guo et al., 2021; Io et al., 2021; Liu et al., 2020; Wei et al.,  
87 2021; Yanagida et al., 2021). In this study, we derived patient-specific human TS cell lines from clinically  
88 available CVS tissue. Derivation of TS cell lines from CVS tissue expands the genetic diversity of  
89 available human TS cells and importantly is linked to clinical data describing pregnancy outcomes.

90

91

## 92 **Results**

### 93 **Derivation of TS cells from CVS biopsies**

94 CVS biopsies were acquired with patient consent as part of standard medical care. Surplus tissue  
95 fragments not used for clinical genetic testing were cultured using modified human TS cell conditions  
96 (**Fig. 1A**). Tissue pieces attached to type IV collagen-coated tissue culture treated plates (**Fig. 1B**). Cell  
97 outgrowths were evident at sites of attachment and expanded over the first several weeks of culture  
98 (**Supplementary Fig 1**). Cells and tissue fragments were passaged prior to reaching confluency and  
99 replated in 24 well plates. Cell colonies emerged after first passage and steadily expanded with culture  
100 medium changes every two days. Colony morphology and growth rates were heterogeneous for the first  
101 few passages but became more homogenous thereafter. The morphology of CVS tissue-derived TS

102 (TS<sup>CV</sup>) cells was consistent with the morphology of cytotrophoblast-derived TS cells (TS<sup>CT</sup>; **Fig. 1B, 2A**).  
103 TS<sup>CV</sup> cell line expansion was carried out slowly to reduce clonal pressure on derived cells. Cell lines were  
104 slowly transitioned into 6 well and 10 cm plate formats after passages 3-4 and 7-8, respectively  
105 (**Supplementary Fig. 1**). Newly established cell lines were cryopreserved beginning at passage 6.  
106 Importantly, TS<sup>CV</sup> cells tolerated cryopreservation. Revived cells survived, attached, and proliferated for  
107 further expansion. Overall, TS<sup>CV</sup> cell line derivation required approximately three months from sample  
108 acquisition to functional assessments of derived lines.

109  
110 The success rate of TS<sup>CV</sup> line derivation was 50%, with five TS<sup>CV</sup> lines (3 XY; 2 XX) successfully  
111 derived from 10 unique patient tissue specimens (6 XY; 4 XX; **Table 1**). Success in cell line derivation  
112 may be impacted by the negative consequences of overnight shipping or the cellular contents of the  
113 tissue fragments but did not appear to be associated with the clinical karyotype of the CVS specimens.  
114 Maternal age range was 31-46 with a mean age of 37.5 years and race was predominantly  
115 white/Caucasian and non-Hispanic/Latino ethnicity. Maternal and paternal ancestries were varied (**Table**  
116 **1**). CVS tissue specimen collection ranged from 10-14 weeks gestation with an average gestational age  
117 of 12 weeks, 3 days (87 days; **Table 1**). The earliest sample was collected at 10 weeks, 6 days gestation  
118 and the latest sample was collected at 13 weeks, 6 days gestation. The amount of starting tissue ranged  
119 from 5-20 mg with a mean of 9.1 mg of tissue (**Table 1**). Clinical genetics performed on tissue specimens  
120 at the time of CVS indicated that five samples had normal karyotypes (4 samples 46, XY and 1 sample  
121 46, XX). Clinical karyotyping of the remaining five samples reported genomic abnormalities including two  
122 samples with trisomy 18 (47, XX, +18 and 47, XY, +18), one sample with trisomy 21 (47, XX, +21), and  
123 two samples with chromosomal translocations (**Table 1**). The five derived TS<sup>CV</sup> cell lines were from three  
124 samples with clinically normal karyotypes (TS<sup>CVK01</sup>, TS<sup>CVK05</sup>, and TS<sup>CVK09</sup>), one with trisomy 21 (TS<sup>CVK08</sup>)  
125 and one with a translocation (TS<sup>CVK07</sup>). Karyotyping was repeated on TS<sup>CV</sup> cells following line derivation  
126 and expansion. Cell line karyotypes were largely consistent with the clinical karyotyping (**Table 1**).  
127 Karyotypes of TS<sup>CVK01</sup>, TS<sup>CVK05</sup>, and TS<sup>CVK08</sup> lines displayed complete consistency with the clinical result.  
128 TS<sup>CVK07</sup> and TS<sup>CV-K09</sup> cell lines exhibited mosaicism. The karyotype for TS<sup>CVK07</sup> reflected the translocation  
129 between chromosomes 11 and 22 identified during clinical assessment in addition to other anomalies

130 reported in a smaller subset of cells. Forty percent of the cells karyotyped for TS<sup>CVK09</sup> were 46, XY. The  
131 remaining 60% of cells analyzed displayed other genetic anomalies, however each individual anomaly  
132 was restricted to 1-2 total cells (**Table 1**).

133

#### 134 **Characterization of TS<sup>CV</sup> cells in the stem state**

135 TS<sup>CT27</sup> (XX) and TS<sup>CT29</sup> (XY) served as reference standard human TS cell lines (Okae et al.,  
136 2018) used for comparative characterization of the TS<sup>CV</sup> cell lines. TS<sup>CV</sup> cells were maintained in a  
137 stem/proliferative state and propagated beyond the Hayflick limit of 50 cell divisions for non-stem cells,  
138 which is consistent with TS<sup>CT</sup> cell proliferation (Okae et al., 2018). All established TS<sup>CV</sup> cell lines were  
139 assessed for presence of mycoplasma by quantitative polymerase chain reaction (**qPCR**) and no  
140 evidence of contamination was detected. TS<sup>CV</sup> cells in the stem state grew in discrete colonies and  
141 displayed a cobblestone morphology, consistent with the morphology of cytotrophoblast-derived cell lines,  
142 TS<sup>CT27</sup> and TS<sup>CT29</sup> (Okae et al., 2018) (**Fig. 2A**). TS<sup>CV</sup> cells displayed additional characteristics consistent  
143 with their trophoblast cell identity (Lee et al., 2016), including expression of microRNAs from the  
144 Chromosome 19 microRNA cluster (**Fig. 2B; C19MC**; hsa-miR-517a-3p and hsa-miR-526b-3p) and  
145 hypomethylation of the E74 Like ETS Transcription Factor 5 (**ELF5**) promoter relative to induced  
146 pluripotent stem (**iPS**) cells (**Fig. 2C**). Overall, TS<sup>CV</sup> and TS<sup>CT</sup> cells cultured in the stem state displayed  
147 similar proliferative, morphologic, microRNA expression, and methylation properties.

148

#### 149 **Analysis of the differentiation capacity of TS<sup>CV</sup> cells**

150 Comparisons of TS<sup>CV</sup> and TS<sup>CT</sup> cell capacities for differentiation into STB and EVT cell lineages,  
151 were performed following cell line derivation (**Supplementary Fig. 1**). Assessments of cell differentiation  
152 were routinely performed following 10 passages. Differentiation was assessed at morphological and  
153 functional levels.

154

155 **STB differentiation.** The ability of TS<sup>CV</sup> cells to differentiate into STB was assessed using the  
156 previously described three-dimensional STB (**ST3D**) protocol (Okae et al., 2018). STB differentiation  
157 elicited significant morphological changes, including the formation of suspended spheroid cell clusters

158 **(Fig. 3A)**. Complementary to the morphological changes observed, TS<sup>CV</sup>-derived STB displayed  
159 downregulation of stem state transcripts *TEAD4*, *LRP2*, and *LIN28A* (**Fig. 3B**) and upregulation of STB  
160 lineage-specific transcripts, including cytochrome P450 Family 11 Subfamily 1 (*CYP11A1*), chorionic  
161 gonadotropin beta 7 (*CGB7*), and syndecan 1 (*SDC1*; **Fig. 3C**). Overall, all TS<sup>CV</sup>-derived STB showed  
162 similar morphological and expression patterns of signature STB transcripts observed in TS<sup>CT</sup>-derived  
163 STB. STB cell differentiation was also attainable in both TS<sup>CV</sup> lines possessing abnormal karyotypes.  
164 Cyst-like STB morphology was evident in TS<sup>CVK07</sup> cells (**Supplementary Fig. 2A**) and TS<sup>CVK08</sup> cells  
165 (**Supplementary Fig. 2B**). *CYP11A1*, *CGB7*, and *SDC1* were upregulated in TS<sup>CVK07</sup> STB and TS<sup>CVK08</sup>  
166 STB compared to the stem state (**Supplementary Fig. 2C, 2D**).

167  
168 **EVT cell differentiation.** Canonical features of EVT cell differentiation observed in TS<sup>CT</sup> cells  
169 were evident in a subset of TS<sup>CV</sup> cell lines possessing a normal karyotype (TS<sup>CVK01</sup> and TS<sup>CVK09</sup>),  
170 including elongated cell morphology (**Fig. 4A; Videos 1-3**) and expression of major histocompatibility  
171 complex, class I, G (*HLA-G*) protein (**Fig. 4B**). EVT cells displayed downregulation of stem state  
172 transcripts *TEAD4*, *LRP2*, and *LIN28A* (**Fig. 4C**). Characteristic EVT transcripts were upregulated,  
173 including *HLA-G*, matrix metalloproteinase 2 (*MMP2*), and C-C motif chemokine receptor 1 (*CCR1*; **Fig.**  
174 **4D**). Overall, these TS<sup>CV</sup> stem cell derived EVT cells were comparable to EVT cells derived from TS<sup>CT</sup>  
175 cells. TS<sup>CVK08</sup>, possessing trisomy 21, was also capable of EVT cell differentiation (**Supplementary Fig.**  
176 **3A-C**). Optimal EVT cell differentiation was not attainable in TS<sup>CVK05</sup> cells (**Supplementary Fig. 4A-C**),  
177 which possesses a normal karyotype, and TS<sup>CVK07</sup> cells, which possesses an abnormal karyotype  
178 (**Supplementary Fig. 4D-F**). Variability in the capacity for human TS cell line differentiation into EVT cells  
179 has been previously reported (Cinkornpumin et al., 2020; Haider et al., 2022; Okae et al., 2018; Shannon  
180 et al., 2022).

181

## 182 **Transcriptomic analysis of the developmental potential of TS<sup>CV</sup> cells**

183 To obtain a broad and unbiased comparative assessment of TS<sup>CV</sup> and TS<sup>CT</sup> in stem, STB, and  
184 EVT differentiated cell states, transcriptomes were captured using RNA-sequencing (**RNA-seq**). Principal  
185 component analysis of all TS<sup>CT</sup> and TS<sup>CV</sup> cell lines identified three primary cell-state specific clusters (**Fig.**

186 **5A)**. Two outliers that did not cluster within a specific cell state were TS<sup>CVK05</sup> and TS<sup>CVK07</sup> cells cultured to  
187 promote EVT cell differentiation. Correlation analyses performed to compare cell expression profiles  
188 identified comparable transcriptomic changes across TS<sup>CV</sup> and TS<sup>CT</sup> cell lines (**Fig. 5B**).

189  
190 STB differentiation from the stem state resulted in broad changes in gene expression in TS<sup>CT</sup>  
191 cells (**Fig. 5C; Supplementary Table 1**) and TS<sup>CV</sup> cells (**Fig. 5D; Supplementary Table 2**), including  
192 downregulation of stem markers *EPCAM*, *LIN28A*, *LRP2*, *PEG10*, and *TEAD4* and upregulation of STB  
193 markers *CGB2*, *CGB7*, *CYP11A1*, *CYP19A1*, and *SDC1*. STB differentiation-induced changes in gene  
194 expression were consistent between TS<sup>CT</sup> (TS<sup>CT27</sup> and TS<sup>CT29</sup>) and TS<sup>CV</sup> (TS<sup>CVK01</sup>, TS<sup>CVK05</sup>, TS<sup>CVK09</sup>) cells  
195 (R=0.88, p<2.23-16; **Fig. 5E**). TS cells possessing abnormal karyotypes also displayed consistent  
196 clustering for the STB lineage (**Fig. 5A, 5B**). STB gene expression profiles were evident in TS<sup>CVK07</sup>  
197 (**Supplementary Fig. 5A Supplementary Table 3**) and TS<sup>CVK08</sup> (**Supplementary Fig. 5B;**  
198 **Supplementary Table 4**) cells. The STB profiles were consistent with gene expression changes  
199 observed in TS<sup>CT</sup> cells as evidenced by strong correlations with TS<sup>CVK07</sup> (R=0.83, p<2.23-16;  
200 **Supplementary Fig. 5C**) and TS<sup>CVK08</sup> (R=0.84, p<2.23-16; **Supplementary Fig. 5D**) cells. Overall,  
201 independent of karyotype, all TS<sup>CT</sup> and TS<sup>CV</sup> lines could undergo successful STB differentiation.

202  
203 TS<sup>CVK01</sup>, TS<sup>CVK08</sup>, TS<sup>CVK09</sup> cells induced to differentiate into EVT cells clustered with EVT cells  
204 differentiated from TS<sup>CT</sup> cell lines (**Fig. 5A**). In contrast, transcriptomes for TS<sup>CVK05</sup> and TS<sup>CVK07</sup> cells  
205 cultured in conditions promoting EVT cell differentiation clustered independent of stem state, STB and  
206 EVT cell clusters (**Fig. 5A**). EVT cells successfully differentiated from the stem state exhibited broad gene  
207 expression changes in TS<sup>CT</sup> (**Fig. 5F; Supplementary Table 5**) and most TS<sup>CV</sup> cell lines with normal  
208 karyotypes (TS<sup>CVK01</sup> and TS<sup>CVK09</sup>; **Fig. 5G; Supplementary Table 6**). These changes included the  
209 downregulation of stem markers *EPCAM*, *LIN28A*, *LRP2*, *PEG10*, and *TEAD4* and upregulation of EVT  
210 cell markers *CCR1*, *HLA-G*, *ITGA1*, *MMP2*, and *NOTUM*. EVT differentiation-induced changes in gene  
211 expression were consistent between TS<sup>CT</sup> (TS<sup>CT27</sup> and TS<sup>CT29</sup>) and TS<sup>CV</sup> (TS<sup>CVK01</sup> and TS<sup>CVK09</sup>) cells  
212 (R=0.83, p<2.23-16; **Fig. 5H**) as well as between TS<sup>CT</sup> and TS<sup>CVK08</sup> cells (R=0.78, p<2.23-16;  
213 **Supplementary Fig. 6A, B, Supplementary Table 7**), which possess Trisomy 21. EVT cell differentiation



214 was less complete in TS<sup>CVK05</sup> cells (R=0.68, p<2.23-16; **Supplementary Fig. 6C, D; Supplementary**  
215 **Table 8**) and in TS<sup>CVK07</sup> cells (R=0.66, p<2.23-16; **Supplementary Fig. 6E, F; Supplementary Table 9**).

216 In summary, these results indicate that TS<sup>CV</sup> cells are capable of self-renewal and effective  
217 differentiation into both STB and EVT cell lineages and can be considered bonafide TS cells. Differences  
218 were noted in the capacity of some TS<sup>CV</sup> lines for EVT cell differentiation.

219

## 220 **Discussion**

221 Our understanding of placenta development and function has benefitted from the availability of in  
222 vitro model systems. In the human, these model systems have included primary cell and explant cultures,  
223 choriocarcinoma-derived cell lines, and immortalized cell lines (Ringler and Strauss, 1990; Shibata et al.,  
224 2020). Each in vitro approach has had merits but also limitations (Lee et al., 2016; Soares et al., 2018).  
225 About two decades ago, Rossant and colleagues reported a procedure for culturing TS cells from the  
226 mouse (Tanaka et al., 1998). These cells could be maintained in a proliferative stem state or induced to  
227 differentiate. Furthermore TS cells could be reintroduced into blastocysts and shown to possess the  
228 capacity to contribute to mouse placentas (Tanaka et al., 1998). Mouse TS cells became an effective  
229 model system to elucidate gene regulatory networks controlling trophoblast cell differentiation and  
230 placental development (Hada et al., 2022; Hemberger et al., 2020; Latos and Hemberger, 2016; Lee et  
231 al., 2019). Efforts ensued to establish TS cells in other species with some success (Asanoma et al., 2011;  
232 Grigor'eva et al., 2009) but human TS cells represented an enigma (Kunath et al., 2014; Shibata et al.,  
233 2020). Culture protocols for sustaining mouse TS cells were ineffective in the human (Kunath et al.,  
234 2014). The discovery of culture conditions for propagating and differentiating human TS cells represented  
235 a major advancement (Okae et al., 2018). Utilizing these human TS cell culture tools, we have  
236 demonstrated the feasibility of capturing and expanding authentic TS cells from human CVS tissue  
237 specimens.

238

239 The initial human TS cell lines were derived from either blastocysts or first trimester pregnancy  
240 terminations (Okae et al., 2018). These human TS cell lines represent the benchmark for all TS cell lines  
241 subsequently derived. CVS biopsies are an alternative tissue source for deriving TS cells. They are



242 retrieved during the first trimester of pregnancy as part of standard medical care (Adusumalli et al., 2007;  
243 Dong et al., 2003; McIntosh et al., 1993; Pisarska et al., 2016; Stranc et al., 1997; Wang et al., 1994;  
244 Williams et al., 1992, 1987). Thus, CVS-derived TS cell lines can be connected to robust pregnancy  
245 outcome information. Human TS cell lines have also been successfully derived from pluripotent stem cells  
246 (Castel et al., 2020; Cinkornpumin et al., 2020; Dong et al., 2020; Guo et al., 2021; lo et al., 2021; Jang et  
247 al., 2022; Liu et al., 2020; Soncin et al., 2022; Viukov et al., 2022; Wei et al., 2021; Yanagida et al., 2021),  
248 miscarriages (Saha et al., 2020), and most recently from term human placenta (Wang et al., 2022). These  
249 alternative TS cell models are potentially useful tools for investigating trophoblast cell development but  
250 each offer caveats for consideration. Pluripotency is established through extensive genomic  
251 reprogramming (Hanna et al., 2010; Papp and Plath, 2013), which minimizes the impact of the epigenetic  
252 landscape established during pregnancy on the TS cell phenotype. TS cells derived from trophoblast  
253 tissue obtained from miscarriages may best contribute to understanding trophoblast cell-related  
254 mechanisms linked to pregnancy failure and the impact of a failed pregnancy on TS cells. TS cells  
255 recovered from term placental tissue reflect the culmination of events transpiring throughout the duration  
256 of pregnancy. It is reasonable to assume that genetic background and source of trophoblast tissue for TS  
257 derivation will influence TS cell behavior. Culturing TS cells under optimized conditions may normalize  
258 some features attributed to an adverse pregnancy and maternal environment, whereas in other cases the  
259 aberrant behavior may persist. Advantages of using CVS-derived TS cells for investigating trophoblast  
260 cell-gene regulatory networks contributing to placental development are evident.

261  
262 TS cell lines were successfully derived from CVS biopsies possessing both normal and abnormal  
263 karyotypes. These TS cell lines could be interrogated in the stem state and following differentiation into  
264 either STB or EVT. TS cells with a triploid karyotype have also been established from human blastocysts  
265 (Kong et al., 2022). Most recently, trophoblast organoids with abnormal karyotypes have been derived  
266 from CVS biopsies (Schaffers et al., 2022). The true impact of the chromosomal abnormalities on TS cells  
267 and their differentiation into STB or EVT cells will require successful cultivation and characterization of  
268 multiple cell lines possessing the same abnormal karyotype.

269

270 Mosaicism is a characteristic feature of the human placenta (Coorens et al., 2021; Robinson and  
271 Del Gobbo, 2021; Yuen and Robinson, 2011). Trophoblast cells possess a tolerance for karyotypic  
272 abnormalities not evident in the embryo or fetus (Coorens et al., 2021; Shahbazi et al., 2020; Yuen and  
273 Robinson, 2011). Each cotyledon of the placenta exhibits elements of trophoblast cell clonality (Coorens  
274 et al., 2021). Placental mosaicism is manifested in genetic and functional differences among cotyledons  
275 within a human placenta (Coorens et al., 2021; Huang et al., 2009; Rubin et al., 1993; Wang et al., 1993).  
276 Among the TS cell lines derived from CVS biopsies, some exhibited a karyotype consistent with the  
277 karyotype of chorionic villus tissue used for the clinical genetic analysis, whereas others differed. These  
278 tissue biopsies contained a mixture of trophoblast and extraembryonic mesoderm contributions (Aplin and  
279 Jones, 2021). Thus, differences in TS cell versus chorionic villus tissue could be attributed to confined  
280 placental mosaicism or alternatively, linked to an unappreciated consequence of culture conditions  
281 required to establish the TS cell lines.

282

283 In summary, the generation of CVS-derived human TS cell lines expands the genetic diversity of  
284 existing TS cell lines available for basic research, provides an opportunity to associate pregnancy  
285 outcomes with trophoblast function, and will provide insight into the importance of genetic anomalies and  
286 mosaicism in trophoblast cell development.

287

288

## 289 **Materials and Methods**

### 290 **Chorionic villus tissue collections, karyotypic analysis, and clinical phenotyping**

291 Chorionic villus tissue was obtained by highly experienced perinatologists as part of standard  
292 medical care between 10-14 weeks of gestation for clinical genetic diagnosis at Cedars-Sinai Medical  
293 Center (Huang et al., 2009; Pisarska et al., 2016). Clinical cytogenetic analysis was performed on tissue  
294 specimens by direct and long-term culture and reviewed by a team of cytogeneticists (Huang et al.,  
295 2009). Residual trophoblast tissue fragments not required for clinical cytogenetic analysis were  
296 recovered, suspended in Complete TS Cell Medium [DMEM/F12 (11320033, Thermo Fisher Scientific),  
297 100  $\mu$ M 2-mercaptoethanol, 0.2% (vol/vol) fetal bovine serum (**FBS**), 50  $\mu$ M penicillin, 50 U/mL  
298 streptomycin, 0.3% bovine serum albumin (**BSA**, BP9704100, Thermo Fisher Scientific), 1% Insulin-  
299 Transferrin-Selenium-Ethanolamine (**ITS-X**) solution (vol/vol, 51500056, Thermo Fisher Scientific)], 8.5  
300  $\mu$ M L-ascorbic acid (A8960, Sigma-Aldrich), 50 ng/mL epidermal growth factor (**EGF**, E9644, Sigma-  
301 Aldrich), 2  $\mu$ M CHIR99021 (04-0004, Reprocell), 0.5  $\mu$ M A83-01 (04-0014, Reprocell), 1  $\mu$ M SB431542  
302 (04-0010, Reprocell), 800  $\mu$ M valproic acid (P4543, Sigma-Aldrich), and 5  $\mu$ M Y27632 (04-0012-02,  
303 Reprocell)] (Okoe et al., 2018), shipped overnight to the University of Kansas Medical Center, and used  
304 for TS cell derivation. Demographic data was collected from patients and included, parental ages, races  
305 and ethnicities, and ancestry (**Table 1**). All human tissue specimens used for research purposes were  
306 collected following informed written consent, deidentified, and approved by institutional review boards at  
307 both Cedars-Sinai Medical Center and at the University of Kansas Medical Center.

308

### 309 **Derivation of TS cells from CVS tissue specimens**

310 Chorionic villus tissue specimens were placed in 24 well tissue culture-treated dishes coated with  
311 5 mg/mL Corning® mouse type IV collagen (35623, Discovery Labware Inc.) diluted in phosphate  
312 buffered saline (**PBS**). Tissue specimen fragments (3-6 pieces per well) were cultured in 300  $\mu$ L of  
313 Complete TS Cell Medium. Tissue fragments attached within 2-5 days. Medium was replaced with fresh  
314 TS cell culture medium after initial attachment and every two days thereafter. Time to first passage was  
315 unique to each sample and determined by the extent of the outgrowth, but commonly occurred around 21  
316 days post plating. Cells and attached tissue fragments were washed with PBS and detached with TrypLE

317 Express (12604021, Thermo Fisher Scientific). Cell and tissue fragments were replated in human TS cell  
318 culture conditions in a 24 well plate format. Colonies emerged after the first passage. Cells were  
319 maintained in 24 well plate format for 3-5 passages and then expanded into 6 well plate format.

320

### 321 **TS cell culture**

322           Following TS cell derivation, TS cells were cultured in dishes pre-coated with iMatrix511 (1:2000  
323 dilution; NP892-01, Reprocell). TS cells were maintained in a modified Complete TS Cell Medium  
324 [DMEM/F12 (11320033, Thermo Fisher Scientific), 50 µM penicillin, 50 U/mL streptomycin, 0.15% BSA  
325 (BP9704100, Thermo Fisher Scientific), 1% ITS-X solution (vol/vol; 51500056, Thermo Fisher Scientific)],  
326 200 µM L-ascorbic acid (A8960, Sigma-Aldrich), 1% KSR (10828028, Thermo Fisher Scientific), 25 ng/mL  
327 EGF (E9644, Sigma-Aldrich), 2 µM CHIR99021 (04-0004, Reprocell), 5 µM A83-01 (04-0014, Reprocell),  
328 800 µM valproic acid (P4543, Sigma-Aldrich), and 2.5 µM Y27632 (04-0012-02, Reprocell)] (Takahashi et  
329 al., 2019). Cell medium was replaced every two days of culture.

330

### 331 **STB differentiation**

332           To induce STB cell differentiation, TS cells were plated into 6 cm petri dishes at a density of  
333 300,000 cells per dish and cultured in ST3D Medium [DMEM/F12 (11320033, Thermo Fisher Scientific),  
334 50 µM penicillin, 50 U/mL streptomycin, 0.15% BSA (BP9704100, Thermo Fisher Scientific), 1% ITS-X  
335 solution (vol/vol; 51500056, Thermo-Fisher)], 200 µM L-ascorbic acid (A8960, Sigma-Aldrich), 5% KSR  
336 (10828028, Thermo Fisher Scientific), 2.5 µM Y27632 (04-0012, Reprocell), 2 µM forskolin (F6886,  
337 Sigma), and 50 ng/mL of EGF (E9644, Sigma)] (Okoe et al., 2018). On day 3 of cell differentiation, 3 mL  
338 of fresh ST3D medium was added to the culture dishes. Cells were analyzed on day 6 of STB cell  
339 differentiation.

340

### 341 **EVT cell differentiation**

342           EVT cell differentiation was induced by plating human TS cells onto 6-well plates pre-coated with  
343 1 µg/mL of mouse type IV collagen at a density of 80,000 cells per well. Cells were cultured in EVT  
344 Differentiation Medium [DMEM/F12 (11320033, Thermo Fisher Scientific), 100 µM 2-mercaptoethanol,

345 0.2% (vol/vol) FBS, 50  $\mu$ M penicillin, 50 U/mL streptomycin, 0.3% bovine serum albumin (BP9704100,  
346 Thermo Fisher Scientific), 1% Insulin-Transferrin-Selenium-Ethanolamine solution (vol/vol; 51500056,  
347 Thermo Fisher Scientific)], 100 ng/mL of neuregulin 1 (**NRG1**, 5218SC, Cell Signaling, Danvers, MA), 7.5  
348  $\mu$ M A83-01 (04-0014, Reprocell, Beltsville, MD), 2.5  $\mu$ M Y27632 (04-0012, Reprocell), 4% KnockOut  
349 Serum Replacement (**KSR**, 10828028, Thermo Fisher Scientific), and 2% Matrigel<sup>®</sup> (CB-40234, Thermo  
350 Fisher Scientific). On day 3 of EVT cell differentiation, the medium was replaced with EVT Differentiation  
351 Medium excluding NRG1 and with a reduced Matrigel<sup>®</sup> concentration of 0.5%. On day 6 of EVT cell  
352 differentiation, the medium was replaced with EVT Differentiation Medium with a Matrigel concentration of  
353 0.5% and excluding NRG1 and KSR. Cells were analyzed on day 8 of EVT cell differentiation.

354

### 355 **Cell line karyotyping**

356 Chromosome analysis of TS<sup>CV</sup> cells was performed using standard cytogenetic methods (Huang  
357 et al., 2009; Pisarska et al., 2016). GTG banded chromosomes were analyzed at 450-550 band levels.  
358 Cytogenetic and FISH results were described according to the current International Standing Committee  
359 on Human Cytogenetic Nomenclature (International Standing Committee on Human Cytogenetic  
360 Nomenclature et al., 2009).

361

### 362 **Immunocytochemical analysis**

363 Cells were fixed with 4% paraformaldehyde (Sigma-Aldrich) for 15 min at room temperature.  
364 Fixed cells were incubated with primary antibody against HLA-G (ab52455, Abcam), followed by  
365 Alexa488-conjugated goat-anti-mouse immunoglobulin G (**IgG**; A32723, Thermo Fisher Scientific)  
366 secondary antibody and 4',6-diamidino-2-phenylindole (**DAPI**; Molecular Probes). Fluorescence images  
367 were captured on a Nikon 80i upright microscope (Nikon) with a Photometrics CoolSNAP-ES  
368 monochrome camera (Roper).

369

### 370 **Pluripotent stem cell culture**

371 Human induced pluripotent stem (**iPS**) cells were cultured in tissue culture plates pre-coated with  
372 Matrigel (1:100 dilution; 356231, Corning). iPS cells were maintained in complete iPS Cell Medium

373 [mTeSR1 Basal Medium + mTeSR1 5X Supplement (85850, STEMCELL) and 10  $\mu$ M Y27632 (04-0012-  
374 02, Reprcell)] and incubated at 37°C and 5% CO<sub>2</sub>. After the first day of culture, cells were cultured in  
375 complete iPS cell medium without Y27632. Medium was replaced every other day of culture. Cells were  
376 passaged or harvested at 80% confluency.

377

### 378 **miRNA isolation, cDNA preparation, and quantitative real-time PCR**

379 Total RNA was isolated using mirVana kit (AM1560, Thermo Fisher Scientific), and RNA  
380 concentration was measured with the Qubit™ RNA BR Assay Kit (Thermo Fisher Scientific). cDNA  
381 synthesis was performed with TaqMan® Advanced miRNA cDNA Synthesis kit (A28007, Thermo Fisher  
382 Scientific). RT-qPCR was performed using TaqMan™Fast Advanced Master Mix (4444556, Thermo  
383 Fisher Scientific) and targeted miRNAs MIR517a-3p, MIR-526b-3p, and housekeeping miRNA MIR103a-  
384 3p (479485\_mir, 478996\_mir, and 478253\_mir; TaqMan™ Advanced miRNA Assays, Thermo Fisher  
385 Scientific; **Supplementary Table 10**). Relative expression of each transcript was calculated using  $\Delta\Delta$ CT  
386 method and normalized to hsa-miR-103a-3p.

387

### 388 **Methylation Analysis**

389 Genomic DNA was isolated using the DNeasy Blood and Tissue Kit (69504, Qiagen), and 500 ng  
390 of DNA was bisulfite converted using the EZ DNA Methylation-Gold Kit (D5005, Zymo Research)  
391 according to instructions. Following bisulfite conversion, the ELF5 promoter region was amplified using a  
392 nested PCR approach with previously reported primers (Primer Set A: forward: 5'-  
393 GGAAATGATGGATATTGAATTTGA-3'; reverse: 5'-CAATAAAAATAAAAACACCTATAACC-3' Primer Set  
394 B: forward: 5'-GAGGTTTTAATATTGGGTTTATAATG-3'; reverse: 5'-  
395 ATAAATAACACCTACAAACAAATCC-3'; **Supplementary Table 11; Lee et al., 2016; Soncin et al.,**  
396 **2022**). PCR was performed with a hot start DNA polymerase, ZymoTaq (E2001, Zymo Research). After  
397 the second PCR, Taq polymerase-amplified PCR products were gel-purified with QIAquick Gel Extraction  
398 Kit (28706X4, Qiagen), using manufacturer protocols. The purified DNA was inserted directly into a  
399 plasmid vector using TOPO® TA Cloning® Kits for Sequencing (450030, Thermo Fisher Scientific)  
400 according to manufacturer instructions. One microliter of purified PCR product was cloned into the

401 plasmid vector (pCR™4-TOPO®) for 5 min at room temperature. Competent *E. coli* were transformed  
402 with the pCR4-TOPO construct, cultured, and minipreps were prepared using the QIAprep Spin Miniprep  
403 Kit (27106X4, Qiagen). Purified DNA was sequenced (Genewiz).

404

#### 405 **RNA isolation and RT-qPCR**

406 Total RNA was isolated using TRIzol®/chloroform precipitation (15596018, Thermo Fisher  
407 Scientific) as previously reported (Varberg et al., 2021). cDNA was synthesized from 1 µg of total RNA  
408 using the High-Capacity cDNA Reverse Transcription Kit (4368813, Thermo Fisher Scientific) and diluted  
409 10 times with ultra-pure distilled water. qPCR was performed using PowerSYBR® Green PCR Master Mix  
410 (4367659, Thermo Fisher Scientific) and primers (250 nM each). RT-qPCR primer sequences are  
411 presented in **Supplementary Table 12**. Amplification and fluorescence detection were measured with a  
412 QuantStudio 5 Flex Real-Time PCR System (Thermo Fisher Scientific). An initial step (95°C, 10 min)  
413 preceded 40 cycles of a two-step PCR (92°C, 15 s; 60°C, 1 min) and was followed by a dissociation step  
414 (95°C, 15 s; 60°C, 15 s; 95°C 15 s). The comparative cycle threshold method was used for relative  
415 quantification of the amount of mRNA for each sample normalized to the housekeeping genes *B2M* or  
416 *POLR2A*.

417

#### 418 **RNA library preparation and RNA-Seq**

419 Stranded mRNA-sequencing was performed on the Illumina NovaSeq 6000 Sequencing  
420 System in the Genomics Core at the University of Kansas Medical Center. Quality control was  
421 completed with the RNA Screen Tape Assay kit (5067-5576, Agilent Technologies) on the Agilent  
422 TapeStation 4200. Total RNA (1 µg) was processed in the following steps: i) oligo dT bead  
423 capture of mRNA, ii) fragmentation, iii) reverse transcription, iv) cDNA end repair, v) Unique Dual  
424 Index (**UDI**) adaptor ligation, vi) strand selection, and vii) library amplification using the Universal  
425 Plus mRNA-Seq with NuQuant library preparation kit (0520-A01, Tecan Genomics). Library  
426 validation was performed with the D1000 Screen Tape Assay kit (5067-5582, Agilent) on the  
427 Agilent Tape Station 4200. Library concentrations were determined with the NuQuant module  
428 using a Qubit 4 Fluorometer (Thermo Fisher Scientific). Libraries were pooled based on equal



429 molar amounts and the multiplexed pool was quantified, in triplicate, using the Roche  
430 Lightcycler96 with FastStart Essential DNA Green Master (06402712001, Roche) and KAPA  
431 Library Quant (Illumina) DNA Standards 1-6 (KK4903, KAPA Biosystems). Using the qPCR  
432 results, the RNA-Seq library pool was adjusted to 2.125 nM for multiplexed sequencing. Pooled  
433 libraries were denatured with 0.2 N NaOH (0.04N final concentration), neutralized with 400 mM  
434 Tris-HCl, pH 8.0, and diluted to 425 pM. Onboard clonal clustering of the patterned flow cell was  
435 performed using the NovaSeq 6000 S1 Reagent Kit (200 cycle, 20012864, Illumina). A 2x101  
436 cycle sequencing profile with dual index reads was completed using the following sequence  
437 profile: Read 1 – 101 cycles x Index Read 1 – 8 cycles x Index Read 2 – 8 cycles x Read 2 – 101  
438 cycles. Sequence data were converted from .bcl to FASTQ file format using bcl2fastq software  
439 and de-multiplexed. Raw FASTQ files were trimmed using default parameters (-r 0.1 -d 0.03) in  
440 Skewer (Version 0.2.2) and reads shorter than 18 bp were discarded. Transcripts were quantified  
441 using Kallisto (Version 0.46.2). Differentially expressed genes (FDR of 0.05) were discovered  
442 using the Bioconductor package DESeq2 in R (Version 1.32.0).

443

#### 444 **Live cell imaging**

445 Cells were placed into an EVOS Onstage Incubator attached to an EVOS FL Automated Imaging  
446 System (Thermo Fisher Scientific). The live cell chamber was maintained at constant temperature (37°C),  
447 humidity, and 5% CO<sub>2</sub>. For stem culture, TS cells were maintained in stem state culture conditions  
448 described above and images were acquired 1-2 days after passage and immediately following culture  
449 medium change. EVT cell differentiation was induced as described above. On the fourth day of the EVT  
450 cell differentiation protocol, cells were placed into the live cell chamber. Phase contrast images were  
451 acquired every 10 min continuously from days 2-4 of stem cell growth or day 4-6 of EVT cell  
452 differentiation.

453

#### 454 **Mycoplasma testing**

455 Mycoplasma presence was assessed using the LookOut® Mycoplasma qPCR Detection Kit  
456 (MP0040A, Sigma-Aldrich). Kit protocols were followed as described.

457

458 **Statistical analysis**

459 Statistical analysis was completed with the GraphPad Prism 9 software. Welch's *t* tests, Brown-  
460 Forsythe and Welch ANOVA tests were applied when appropriate. The figures depict the data  
461 represented as mean  $\pm$  standard deviation with a statistical significance level of  $p < 0.05$ .

462

463 **Acknowledgements**

464 We thank Stacy Oxley and Brandi Miller for their assistance.

465

466 **Author contributions**

467 K.M.V., M.D.P, and M.J.S. conceived and designed the research; A.N., J.W., and M.D.P. collected and  
468 obtained tissue specimens. J.G., I.S., H.O., and T.A. provided reagents, protocols, or equipment; K.M.V.,  
469 A.M., B.K., and B.M., performed experiments and/or analyzed data; K.M.V, A.M., J.G, I.S., E.G., M.D.P,  
470 and M.J.S. interpreted results of experiments; K.M.V., A.M., J.M.V., and M.J.S. prepared figures and  
471 drafted manuscript; K.M.V. M.D.P, and M.J.S. edited and revised manuscript; All authors approved final  
472 version of manuscript.

473

474 **Ethics**

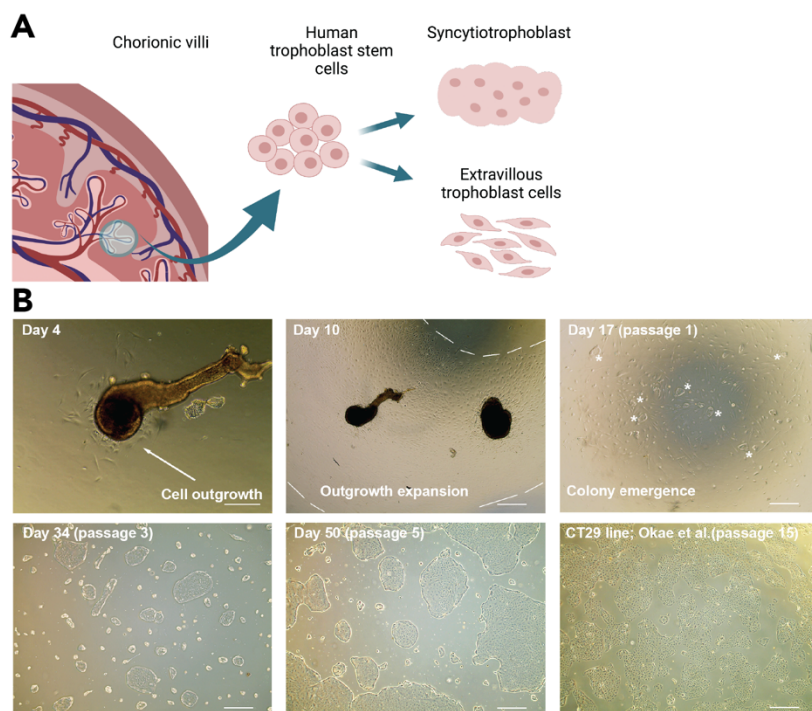
475 There is no conflict of interest that could be perceived as prejudicing the impartiality of the research  
476 reported.

477

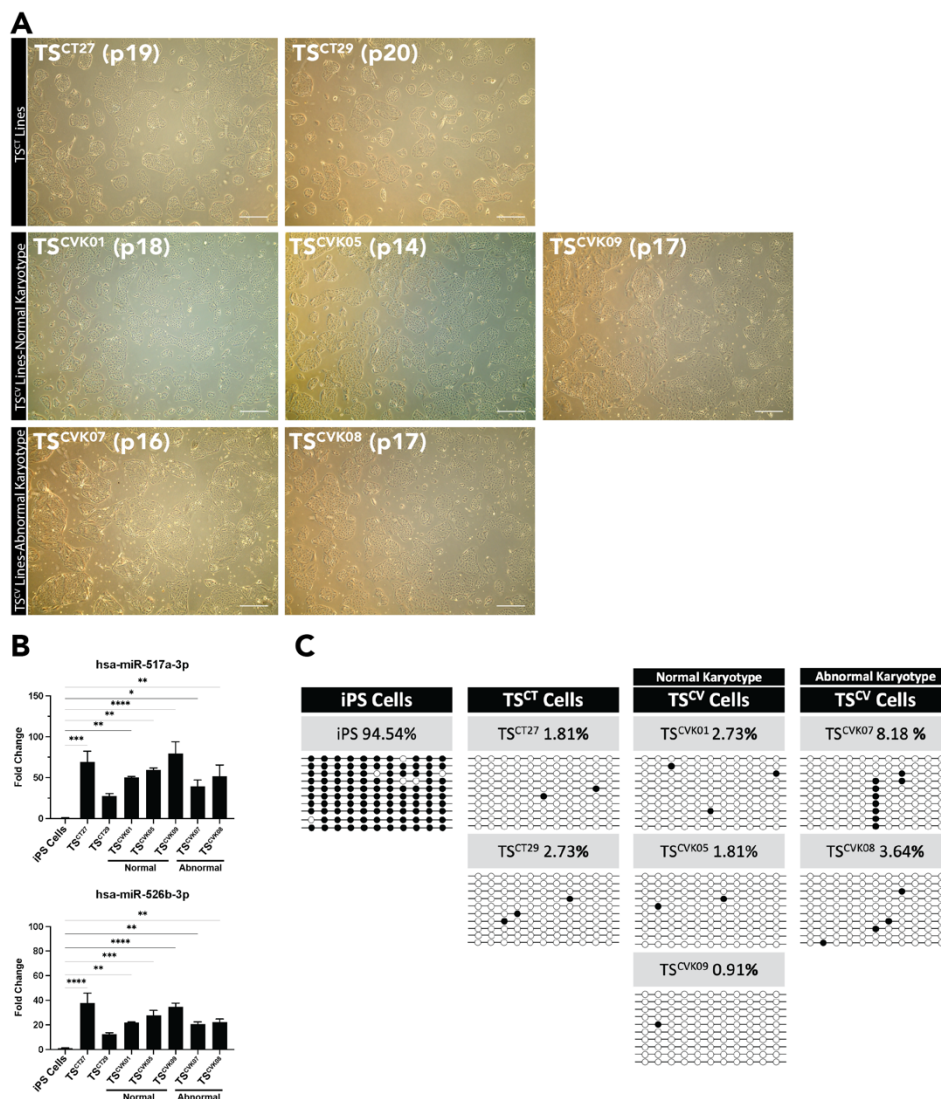
478 **Data availability**

479 All raw and processed sequencing data generated in this study have been submitted to the NCBI Gene  
480 Expression Omnibus (GEO; [\(\)](#) under accession number GSE #).

481 **Tables and Figures**

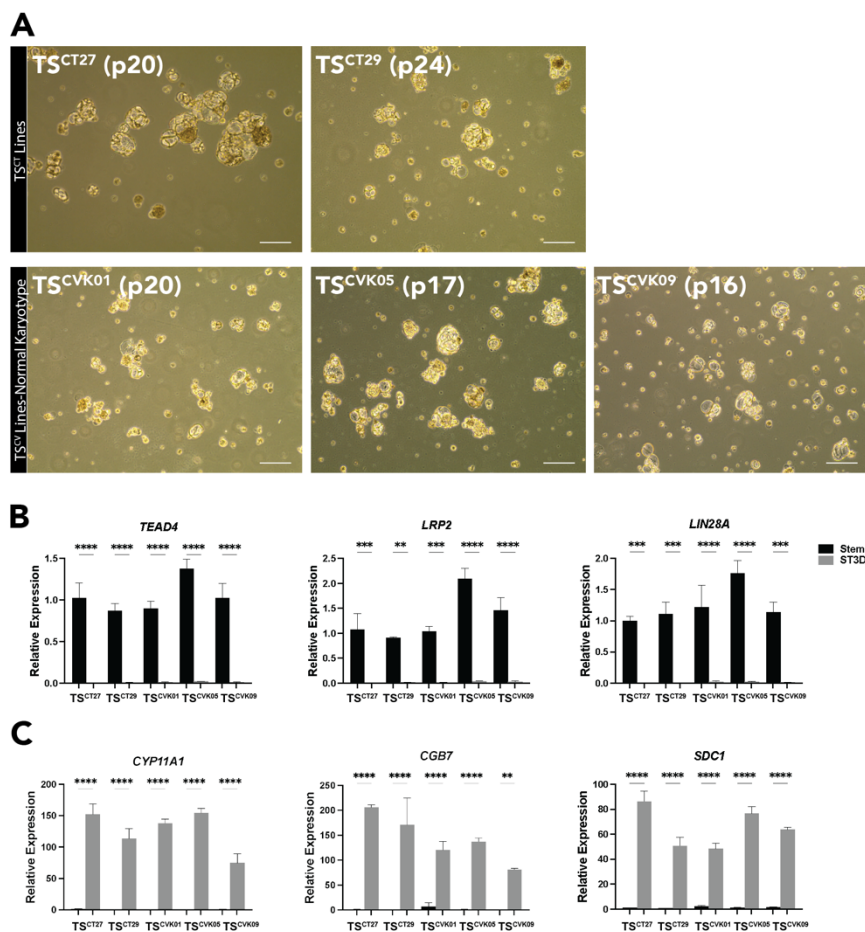


482 **Fig. 1 Deriving TS cells from CVS tissue specimens. A)** Simplified schematic depicting the process of  
483 obtaining chorionic villi tissue fragments, derivation of TS cells, and then subsequent differentiation into  
484 STB and EVT cell lineages. Created with BioRender.com. **B)** Chorionic villus tissue fragments attach and  
485 form cellular outgrowths within a few days of initial plating. Within one to two weeks the outgrowths  
486 expand and proliferate across the well. Two to three weeks after plating, the cells were passaged, and  
487 colonies emerged. Colony clusters were initially small but proliferated and grew rapidly. Significant  
488 heterogeneity is present initially, but subsequent passaging selects for a TS cell population that displays a  
489 similar morphology to the original TS cell lines (Okae et al., 2018), which possess the ability to  
490 differentiate into STB and EVT cell lineages. Scale bar represents 250  $\mu\text{m}$  in first panel. All other scale  
491 bars represent 500  $\mu\text{m}$ .



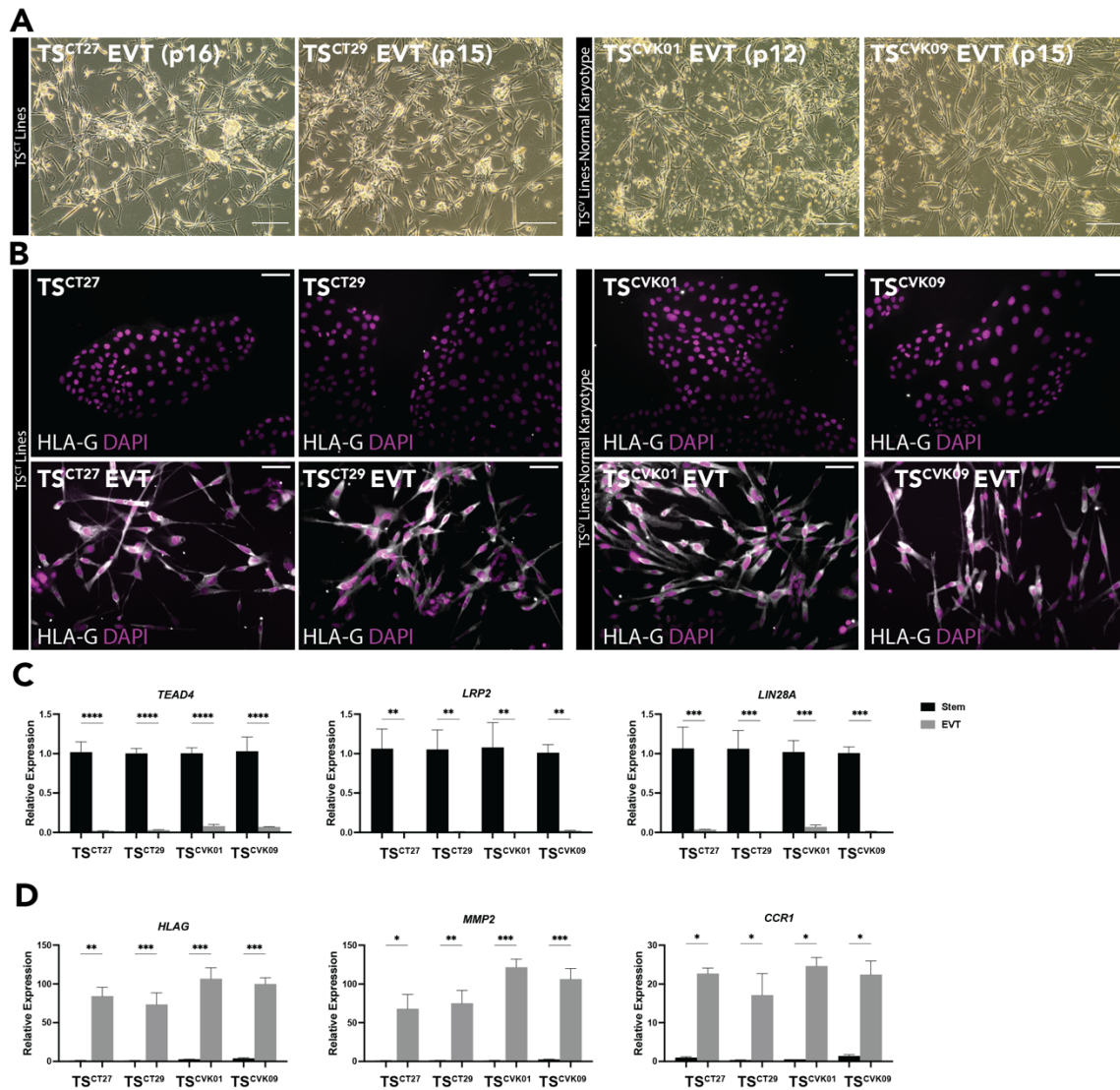
492

493 **Fig. 2 Characterization of TS<sup>CV</sup> cells. A)** Stem state phase contrast images of the five CVS-derived TS  
 494 cell lines (TS<sup>CVK01</sup>, TS<sup>CVK05</sup>, TS<sup>CVK07</sup>, TS<sup>CVK08</sup>, TS<sup>CVK09</sup>) alongside images of the reference cytotrophoblast-  
 495 derived TS cell lines (TS<sup>CT27</sup> and TS<sup>CT29</sup>) at different passage numbers (14-20). Scale bars represent 500  
 496  $\mu\text{m}$ . **B)** Bar graphs depicting expression of two microRNAs (miR) from the C19MC cluster (hsa-miR-517a-  
 497 3p and hsa-miR-526b-3p) in TS<sup>CT</sup> and TS<sup>CV</sup> cell lines relative to induced pluripotent stem (iPS) cells,  
 498 measured by RT-qPCR. Data were normalized to the control miRNA, hsa-miR-103a-3p (n=3 samples per  
 499 group; \*p<0.05, \*\*p<0.01, \*\*\*p<0.001, \*\*\*\*p<0.0001). **C)** Plots representing DNA methylation levels in the  
 500 ELF5 promoter at 11 sites in TS<sup>CT</sup> and TS<sup>CV</sup> cell lines compared to iPS cells. Methylated sites (black) and  
 501 unmethylated sites (white) are shown for 10 replicates and the average percent methylation is listed.



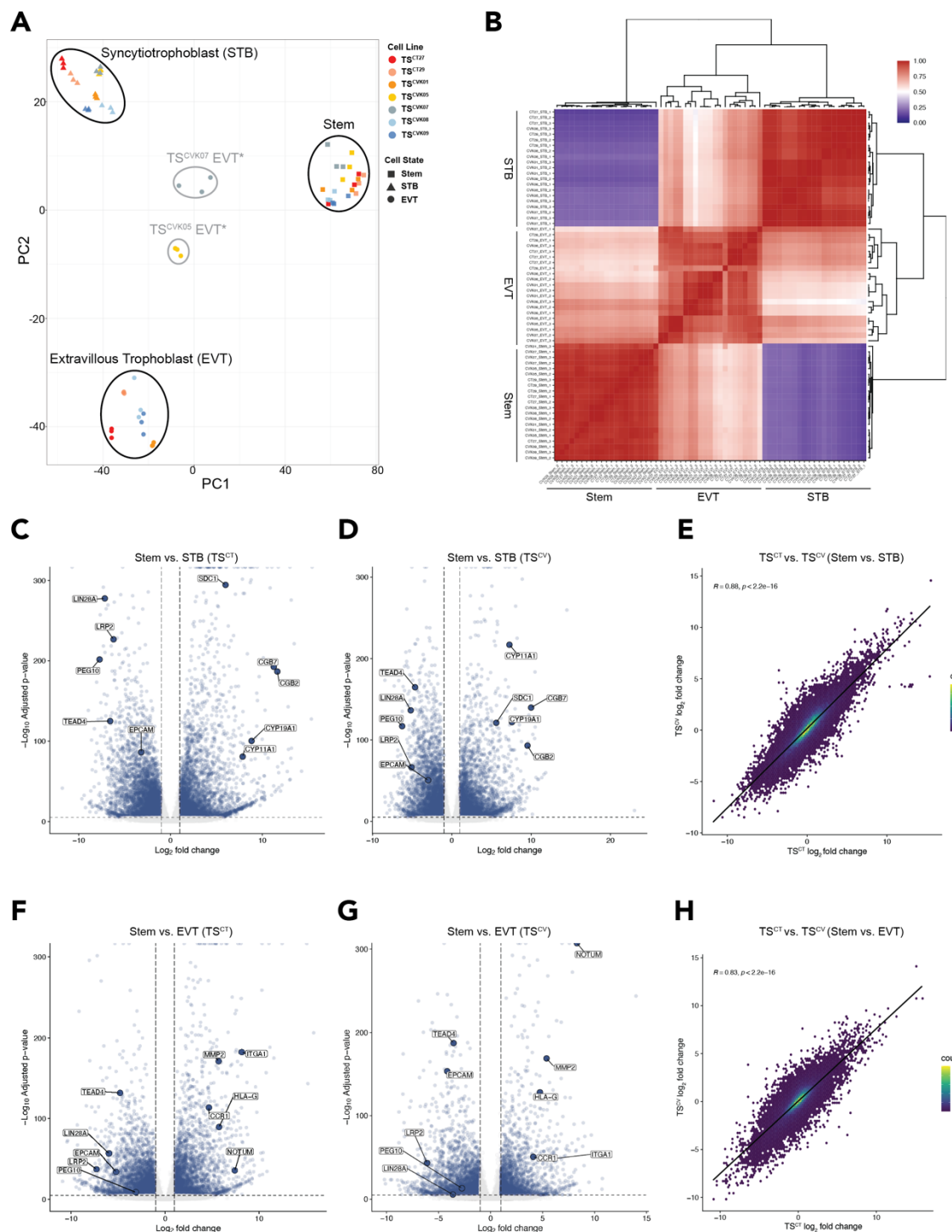
502 **Fig. 3 TS<sup>CV</sup> cell line differentiation into STB.** **A)** Representative phase contrast images of  
 503 cytotrophoblast-derived TS<sup>CT27</sup> and TS<sup>CT29</sup> cells and three CVS-derived TS cell lines possessing a normal  
 504 karyotype, TS<sup>CVK01</sup>, TS<sup>CVK05</sup>, and TS<sup>CVK09</sup>, cultured under STB differentiation conditions. Scale bars  
 505 represent 250  $\mu$ m. **B-C)** Stem cell-specific transcripts (**B**; *TEAD4*, *LRP2*, and *LIN28A*) and STB cell-  
 506 specific transcripts (**C**; *CYP11A1*, *CGB7*, and *SDC1*) were quantified by RT-qPCR in stem (black) and  
 507 STB differentiated (gray) TS<sup>CT27</sup>, TS<sup>CT29</sup>, TS<sup>CVK01</sup>, TS<sup>CVK05</sup>, and TS<sup>CVK09</sup> cells (n=3 samples per group;  
 508 \*\*p<0.01, \*\*\*p<0.001, \*\*\*\*p<0.0001).





509 **Fig. 4 TS<sup>CV</sup> cell line differentiation into EVT cells.** **A)** Representative phase contrast images of  
 510 cytotrophoblast-derived TS<sup>CT27</sup> and TS<sup>CT29</sup> cells and two CVS-derived TS cell lines possessing a normal  
 511 karyotype, TS<sup>CVK01</sup> and TS<sup>CVK09</sup>, cells cultured under EVT cell differentiation conditions. Scale bars  
 512 represent 250  $\mu$ m **B)** Immunofluorescence detection of HLA-G (gray) by immunocytochemistry in TS<sup>CT</sup>  
 513 and TS<sup>CV</sup> cells cultured in the stem state and on day 8 of EVT cell differentiation. DAPI (magenta) stains  
 514 cell nuclei. Scale bars represent 100  $\mu$ m. **C-D)** Stem cell-specific transcripts (**C**; *TEAD4*, *LRP2*, and  
 515 *LIN28A*) and EVT cell-specific transcripts (**D**; *HLA-G*, *MMP2*, and *CCR1*) were quantified by RT-qPCR in  
 516 stem (black) and EVT differentiated (gray) TS<sup>CT27</sup>, TS<sup>CT29</sup>, TS<sup>CVK01</sup> and TS<sup>CVK09</sup> cells (n=3 samples per  
 517 group; \*p<0.05, \*\*p<0.01, \*\*\*p<0.001, \*\*\*\*p<0.0001).

518



519  
 520 **Fig. 5 TS<sup>CV</sup> and TS<sup>CT</sup> cells cluster by cell state and share similar transcriptomes. A)** Principal  
 521 component analysis based on RNA-seq datasets generated from TS<sup>CT</sup> and TS<sup>CV</sup> cells cultured in the stem  
 522 state or following differentiation into STB and EVT cell lineages. **B)** Heat map of Pearson correlation  
 523 coefficients from expression profiles of stem state, STB, and EVT cell lines, with the dendrogram



524 generated by hierarchical clustering. **C-D**) Volcano plots depicting significantly up- and down-regulated  
525 genes based on transcripts measured by RNA-seq in stem versus STB state  $TS^{CT}$  (**C**) and  $TS^{CV}$  (**D**) cells.  
526 Gene transcript levels unchanged between stem and STB state cells are depicted in green (n=3 per  
527 group; absolute log<sub>2</sub>fold change >1, adjusted p<0.05). **E**) Two-dimensional density plot comparing gene  
528 expression changes between stem and EVT cell states in  $TS^{CT}$  ( $TS^{CT27}$  and  $TS^{CT29}$ ) cells versus  $TS^{CV}$   
529 ( $TS^{CVK01}$ ,  $TS^{CVK05}$ , and  $TS^{CVK09}$ ) cells (Pearson correlation coefficient (R)=0.88, p<2.2e-16). **F-G**) Volcano  
530 plots depicting significantly up- and down-regulated genes based on transcripts measured by RNA-seq in  
531 stem versus EVT states of  $TS^{CT}$  (**F**) and  $TS^{CV}$  (**G**) cells. Gene transcript levels unchanged between stem  
532 and EVT state cells are depicted in green (n=3 per group; absolute log<sub>2</sub>fold change >1, adjusted p<0.05).  
533 **H**) Two-dimensional density plot comparing gene expression changes between stem and EVT cell states  
534 in  $TS^{CT}$  ( $TS^{CT27}$  and  $TS^{CT29}$ ) cells versus  $TS^{CV}$  ( $TS^{CVK01}$  and  $TS^{CVK09}$ ) cells (Pearson correlation coefficient  
535 (R)=0.83, p<2.2e-16).

536 **Table 1. CVS Specimen Data.** Descriptive information for ten independent chorionic villus tissue  
537 collections (K01-K10) that were cultured for TS cell derivation. TS<sup>CV</sup> cell lines were successfully  
538 established from five of the chorionic villus tissue specimens (2 XX and 3 XY cell lines). Karyotypic  
539 analysis was performed at the time of CVS collection and in TS<sup>CV</sup> cell lines (after passage 10). Pregnancy  
540 outcomes are presented for each CVS tissue collection as well as select associated maternal and  
541 paternal demographics.

542

543 **Video 1. Stem state and EVT-differentiated TS<sup>CT27</sup> cell growth and motility.** Phase contrast images  
544 were acquired every 10 min for 53 h of TS<sup>CT27</sup> cells cultured under stem state or EVT cell-differentiation  
545 conditions (EVT cell differentiation protocol days 4-6).

546

547 **Video 2. Stem state and EVT cell differentiated TS<sup>CVK01</sup> cell growth and motility.** Phase contrast  
548 images were acquired every 10 min for 53 h of TS<sup>CVK01</sup> cells cultured under stem state or EVT cell  
549 differentiation conditions (EVT cell differentiation protocol days 4-6).

550

551 **Video 3. Stem state and EVT cell differentiated TS<sup>CVK09</sup> cell growth and motility.** Phase contrast  
552 images were acquired every 10 min for 53 h of TS<sup>CVK09</sup> cells cultured under stem state or EVT cell  
553 differentiation conditions (EVT cell differentiation protocol days 4-6).

## 554 References

- 555 Adusumalli J, Han CS, Beckham S, Bartholomew ML, Williams J. 2007. Chorionic villus sampling  
556 and risk for hypertensive disorders of pregnancy. *Am J Obstet Gynecol* **196**:591.e1–7;  
557 discussion 591.e7. doi:10.1016/j.ajog.2007.03.015
- 558 Aplin JD, Jones CJP. 2021. Cell dynamics in human villous trophoblast. *Hum Reprod Update*  
559 **27**:904–922. doi:10.1093/humupd/dmab015
- 560 Asanoma K, Rumi MAK, Kent LN, Chakraborty D, Renaud SJ, Wake N, Lee D-S, Kubota K,  
561 Soares MJ. 2011. FGF4-dependent stem cells derived from rat blastocysts differentiate  
562 along the trophoblast lineage. *Dev Biol* **351**:110–119. doi:10.1016/j.ydbio.2010.12.038
- 563 Bhattacharya B, Home P, Ganguly A, Ray S, Ghosh A, Islam MR, French V, Marsh C,  
564 Gunewardena S, Okae H, Arima T, Paul S. 2020. Atypical protein kinase C iota (PKC*ι*)  
565 ensures mammalian development by establishing the maternal-fetal exchange interface.  
566 *Proc Natl Acad Sci U S A* **117**:14280–14291. doi:10.1073/pnas.1920201117
- 567 Castel G, Meistermann D, Bretin B, Firmin J, Blin J, Loubersac S, Bruneau A, Chevolleau S,  
568 Kilens S, Chariou C, Gaignerie A, Francheteau Q, Kagawa H, Charpentier E, Flippe L,  
569 François-Campion V, Haider S, Dietrich B, Knöfler M, Arima T, Bourdon J, Rivron N,  
570 Masson D, Fournier T, Okae H, Fréour T, David L. 2020. Induction of human trophoblast  
571 stem cells from somatic cells and pluripotent stem cells. *Cell Rep* **33**:108419.  
572 doi:10.1016/j.celrep.2020.108419
- 573 Cinkornpumin JK, Kwon SY, Guo Y, Hossain I, Sirois J, Russett CS, Tseng H-W, Okae H, Arima  
574 T, Duchaine TF, Liu W, Pastor WA. 2020. Naive human embryonic stem cells can give  
575 rise to cells with a trophoblast-like transcriptome and methylome. *Stem Cell Reports*  
576 **15**:198–213. doi:10.1016/j.stemcr.2020.06.003
- 577 Coorens THH, Oliver TRW, Sanghvi R, Sovio U, Cook E, Vento-Tormo R, Haniffa M, Young MD,  
578 Rahbari R, Sebire N, Campbell PJ, Charnock-Jones DS, Smith GCS, Behjati S. 2021.  
579 Inherent mosaicism and extensive mutation of human placentas. *Nature* **592**:80–85.  
580 doi:10.1038/s41586-021-03345-1
- 581 Dong C, Beltcheva M, Gontarz P, Zhang B, Popli P, Fischer LA, Khan SA, Park K-M, Yoon E-J,  
582 Xing X, Kommagani R, Wang T, Solnica-Krezel L, Theunissen TW. 2020. Derivation of  
583 trophoblast stem cells from naïve human pluripotent stem cells. *Elife* **9**:e52504.  
584 doi:10.7554/eLife.52504
- 585 Dong L, Falk RE, Williams J, Kohan M, Schreck RR. 2003. Tetrasomy 12p--unusual presentation  
586 in CVS. *Prenat Diagn* **23**:101–103. doi:10.1002/pd.538
- 587 Flowers AE, Gonzalez TL, Joshi NV, Eisman LE, Clark EL, Buttle RA, Sauro E, DiPentino R, Lin  
588 Y, Wu D, Wang Y, Santiskulvong C, Tang J, Lee B, Sun T, Chan JL, Wang ET, Jefferies  
589 C, Lawrenson K, Zhu Y, Afshar Y, Tseng H-R, Williams J, Pisarska MD. 2021. Sex  
590 differences in microRNA expression in first and third trimester human placenta†. *Biol*  
591 *Reprod* ioab221. doi:10.1093/biolre/ioab221
- 592 Gonzalez TL, Eisman LE, Joshi NV, Flowers AE, Wu D, Wang Y, Santiskulvong C, Tang J, Buttle  
593 RA, Sauro E, Clark EL, DiPentino R, Jefferies CA, Chan JL, Lin Y, Zhu Y, Afshar Y,  
594 Tseng H-R, Taylor K, Williams J, Pisarska MD. 2021. High-throughput  
595 miRNA sequencing of the human placenta: expression throughout gestation.  
596 *Epigenomics* **13**:995–1012. doi:10.2217/epi-2021-0055
- 597 Grigor'eva EV, Shevchenko AI, Mazurok NA, Elisaphenko EA, Zhelezova AI, Shilov AG, Dyban  
598 PA, Dyban AP, Noniashvili EM, Slobodyanyuk SYa, Nesterova TB, Brockdorff N, Zakian  
599 SM. 2009. FGF4 Independent Derivation of Trophoblast Stem Cells from the Common  
600 Vole. *PLoS ONE* **4**:e7161. doi:10.1371/journal.pone.0007161
- 601 Guo G, Stirparo GG, Strawbridge SE, Spindlow D, Yang J, Clarke J, Dattani A, Yanagida A, Li  
602 MA, Myers S, Özel BN, Nichols J, Smith A. 2021. Human naive epiblast cells possess  
603 unrestricted lineage potential. *Cell Stem Cell* **28**:1040-1056.e6.  
604 doi:10.1016/j.stem.2021.02.025
- 605 Hada M, Miura H, Tanigawa A, Matoba S, Inoue K, Ogonuki N, Hirose M, Watanabe N, Nakato R,  
606 Fujiki K, Hasegawa A, Sakashita A, Okae H, Miura K, Shikata D, Arima T, Shirahige K,  
607 Hiratani I, Ogura A. 2022. Highly rigid H3.1/H3.2-H3K9me3 domains set a barrier for cell

- 608 fate reprogramming in trophoblast stem cells. *Genes Dev* **36**:84–102.  
609 doi:10.1101/gad.348782.121
- 610 Haider S, Lackner AI, Dietrich B, Kunihs V, Haslinger P, Meinhardt G, Maxian T, Saleh L, Fiala C,  
611 Pollheimer J, Latos PA, Knöfler M. 2022. Transforming growth factor- $\beta$  signaling governs  
612 the differentiation program of extravillous trophoblasts in the developing human placenta.  
613 *Proc Natl Acad Sci U S A* **119**:e2120667119. doi:10.1073/pnas.2120667119
- 614 Hanna JH, Saha K, Jaenisch R. 2010. Pluripotency and cellular reprogramming: facts,  
615 hypotheses, unresolved issues. *Cell* **143**:508–525. doi:10.1016/j.cell.2010.10.008
- 616 Hemberger M, Hanna CW, Dean W. 2020. Mechanisms of early placental development in mouse  
617 and humans. *Nat Rev Genet* **21**:27–43. doi:10.1038/s41576-019-0169-4
- 618 Hornbachner R, Lackner A, Papuchova H, Haider S, Knöfler M, Mechtler K, Latos PA. 2021.  
619 MSX2 safeguards syncytiotrophoblast fate of human trophoblast stem cells. *Proc Natl*  
620 *Acad Sci U S A* **118**:e2105130118. doi:10.1073/pnas.2105130118
- 621 Huang A, Adusumalli J, Patel S, Liem J, Williams J, Pisarska MD. 2009. Prevalence of  
622 chromosomal mosaicism in pregnancies from couples with infertility. *Fertil Steril* **91**:2355–  
623 2360. doi:10.1016/j.fertnstert.2008.03.044
- 624 International Standing Committee on Human Cytogenetic Nomenclature, Shaffer LG, Slovak ML,  
625 Campbell LJ, editors. 2009. ISCN 2009: an international system for human cytogenetic  
626 nomenclature (2009). Basel ; Unionville, CT: Karger.
- 627 Ito S, Kabata M, Iemura Y, Semi K, Morone N, Minagawa A, Wang B, Okamoto I, Nakamura T,  
628 Kojima Y, Iwatani C, Tsuchiya H, Kaswandy B, Kondoh E, Kaneko S, Woltjen K, Saitou  
629 M, Yamamoto T, Mandai M, Takashima Y. 2021. Capturing human trophoblast  
630 development with naive pluripotent stem cells in vitro. *Cell Stem Cell* **28**:1023-1039.e13.  
631 doi:10.1016/j.stem.2021.03.013
- 632 Ishiuchi T, Ohishi H, Sato T, Kamimura S, Yorino M, Abe S, Suzuki A, Wakayama T, Suyama M,  
633 Sasaki H. 2019. Zfp281 shapes the transcriptome of trophoblast stem cells and is  
634 essential for placental development. *Cell Reports* **27**:1742-1754.e6.  
635 doi:10.1016/j.celrep.2019.04.028
- 636 Jaju Bhattad G, Jeyarajah MJ, McGill MG, Dumeaux V, Okae H, Arima T, Lajoie P, Bérubé NG,  
637 Renaud SJ. 2020. Histone deacetylase 1 and 2 drive differentiation and fusion of  
638 progenitor cells in human placental trophoblasts. *Cell Death Dis* **11**:311.  
639 doi:10.1038/s41419-020-2500-6
- 640 Jang YJ, Kim M, Lee B-K, Kim J. 2022. Induction of human trophoblast stem-like cells from  
641 primed pluripotent stem cells. *Proc Natl Acad Sci U S A* **119**:e2115709119.  
642 doi:10.1073/pnas.2115709119
- 643 Knöfler M, Haider S, Saleh L, Pollheimer J, Gamage TKJB, James J. 2019. Human placenta and  
644 trophoblast development: key molecular mechanisms and model systems. *Cell Mol Life*  
645 *Sci* **76**:3479–3496. doi:10.1007/s00018-019-03104-6
- 646 Kong X, Chen X, Ou S, Wang W, Li R. 2022. Derivation of human triploid trophoblast stem cells.  
647 *J Assist Reprod Genet* **39**:1183–1193. doi:10.1007/s10815-022-02436-w
- 648 Kunath T, Yamanaka Y, Detmar J, MacPhee D, Caniggia I, Rossant J, Jurisicova A. 2014.  
649 Developmental differences in the expression of FGF receptors between human and  
650 mouse embryos. *Placenta* **35**:1079–1088. doi:10.1016/j.placenta.2014.09.008
- 651 Latos PA, Hemberger M. 2016. From the stem of the placental tree: trophoblast stem cells and  
652 their progeny. *Development* **143**:3650–3660. doi:10.1242/dev.133462
- 653 Lee B-K, Jang YJ, Kim M, LeBlanc L, Rhee C, Lee J, Beck S, Shen W, Kim J. 2019. Super-  
654 enhancer-guided mapping of regulatory networks controlling mouse trophoblast stem  
655 cells. *Nat Commun* **10**:4749. doi:10.1038/s41467-019-12720-6
- 656 Lee CQE, Gardner L, Turco M, Zhao N, Murray MJ, Coleman N, Rossant J, Hemberger M,  
657 Moffett A. 2016. What is trophoblast? A combination of criteria define human first-  
658 trimester trophoblast. *Stem Cell Reports* **6**:257–272. doi:10.1016/j.stemcr.2016.01.006
- 659 Liu X, Ouyang JF, Rossello FJ, Tan JP, Davidson KC, Valdes DS, Schröder J, Sun YBY, Chen J,  
660 Knaupp AS, Sun G, Chy HS, Huang Z, Pflueger J, Firas J, Tano V, Buckberry S, Paynter  
661 JM, Larcombe MR, Poppe D, Choo XY, O'Brien CM, Pastor WA, Chen D, Leichter AL,  
662 Naeem H, Tripathi P, Das PP, Grubman A, Powell DR, Laslett AL, David L, Nilsson SK,  
663 Clark AT, Lister R, Nefzger CM, Martelotto LG, Rackham OJL, Polo JM. 2020.

- 664 Reprogramming roadmap reveals route to human induced trophoblast stem cells. *Nature*  
665 **586**:101–107. doi:10.1038/s41586-020-2734-6
- 666 McIntosh N, Rubin C, Wang B, Williams J. 1993. Transcervical CVS sample size: correlation with  
667 placental location, cytogenetic findings, and pregnancy outcome. *Prenat Diagn* **13**:1031–  
668 1036. doi:10.1002/pd.1970131105
- 669 Muto M, Chakraborty D, Varberg KM, Moreno-Irusta A, Iqbal K, Scott RL, McNally RP,  
670 Choudhury RH, Aplin JD, Okae H, Arima T, Matsumoto S, Ema M, Mast AE, Grundberg  
671 E, Soares MJ. 2021. Intersection of regulatory pathways controlling hemostasis and  
672 hemochorial placentation. *Proc Natl Acad Sci U S A* **118**:e2111267118.  
673 doi:10.1073/pnas.2111267118
- 674 Okae H, Toh H, Sato T, Hiura H, Takahashi S, Shirane K, Kabayama Y, Suyama M, Sasaki H,  
675 Arima T. 2018. Derivation of human trophoblast stem cells. *Cell Stem Cell* **22**:50–63.e6.  
676 doi:10.1016/j.stem.2017.11.004
- 677 Papp B, Plath K. 2013. Epigenetics of reprogramming to induced pluripotency. *Cell* **152**:1324–  
678 1343. doi:10.1016/j.cell.2013.02.043
- 679 Perez-Garcia V, Lea G, Lopez-Jimenez P, Okkenhaug H, Burton GJ, Moffett A, Turco MY,  
680 Hemberger M. 2021. BAP1/ASXL complex modulation regulates epithelial-mesenchymal  
681 transition during trophoblast differentiation and invasion. *Elife* **10**:e63254.  
682 doi:10.7554/eLife.63254
- 683 Pisarska MD, Akhlaghpour M, Lee B, Barlow GM, Xu N, Wang ET, Mackey AJ, Farber CR, Rich  
684 SS, Rotter JI, Chen YI, Goodarzi MO, Guller S, Williams J. 2016. Optimization of  
685 techniques for multiple platform testing in small, precious samples such as human  
686 chorionic villus sampling. *Prenat Diagn* **36**:1061–1070. doi:10.1002/pd.4936
- 687 Ringler GE, Strauss JF. 1990. In vitro systems for the study of human placental endocrine  
688 function. *Endocr Rev* **11**:105–123. doi:10.1210/edrv-11-1-105
- 689 Robinson WP, Del Gobbo GF. 2021. Mistakes Are Common; Should We Worry about Them?  
690 *Trends Mol Med* **27**:721–722. doi:10.1016/j.molmed.2021.04.008
- 691 Ruane PT, Garner T, Parsons L, Babbington PA, Wangsaputra I, Kimber SJ, Stevens A,  
692 Westwood M, Brison DR, Aplin JD. 2022. Trophoblast differentiation to invasive  
693 syncytiotrophoblast is promoted by endometrial epithelial cells during human embryo  
694 implantation. *Hum Reprod* **37**:777–792. doi:10.1093/humrep/deac008
- 695 Rubin CH, Williams J, Wang BB. 1993. Discrepancy in mosaic findings between chorionic villi and  
696 amniocytes: a diagnostic dilemma involving 45,X, 46,XY, and 47,XYY cell lines. *Am J*  
697 *Med Genet* **46**:457–459. doi:10.1002/ajmg.1320460424
- 698 Saha B, Ganguly A, Home P, Bhattacharya B, Ray S, Ghosh A, Rumi MAK, Marsh C, French VA,  
699 Gunewardena S, Paul S. 2020. TEAD4 ensures postimplantation development by  
700 promoting trophoblast self-renewal: An implication in early human pregnancy loss. *Proc*  
701 *Natl Acad Sci U S A* **117**:17864–17875. doi:10.1073/pnas.2002449117
- 702 Schaffers OJM, Dupont C, Bindels EM, Van Opstal D, Dekkers DHW, Demmers JAA, Gribnau J,  
703 Rijn BB van. 2022. Single-Cell Atlas of Patient-Derived Trophoblast Organoids in  
704 Ongoing Pregnancies. *Organoids* **1**:106–115.  
705 doi:https://doi.org/10.3390/organoids1020009
- 706 Shahbazi MN, Wang T, Tao X, Weatherbee BAT, Sun L, Zhan Y, Keller L, Smith GD, Pellicer A,  
707 Scott RT, Seli E, Zernicka-Goetz M. 2020. Developmental potential of aneuploid human  
708 embryos cultured beyond implantation. *Nat Commun* **11**:3987. doi:10.1038/s41467-020-  
709 17764-7
- 710 Shannon MJ, Baltayeva J, Castellana B, Wächter J, McNeill GL, Yoon JS, Treissman J, Le HT,  
711 Lavoie PM, Beristain AG. 2022. Cell trajectory modeling identifies a primitive trophoblast  
712 state defined by BCAM enrichment. *Development* **149**:dev199840.  
713 doi:10.1242/dev.199840
- 714 Sheridan MA, Zhao X, Fernando RC, Gardner L, Perez-Garcia V, Li Q, Marsh SGE, Hamilton R,  
715 Moffett A, Turco MY. 2021. Characterization of primary models of human trophoblast.  
716 *Development* **148**:dev199749. doi:10.1242/dev.199749
- 717 Shibata S, Kobayashi EH, Kobayashi N, Oike A, Okae H, Arima T. 2020. Unique features and  
718 emerging in vitro models of human placental development. *Reprod Med Biol* **19**:301–313.  
719 doi:10.1002/rmb2.12347



- 720 Soares MJ, Varberg KM, Iqbal K. 2018. Hemochorial placentation: development, function, and  
721 adaptations†. *Biology of Reproduction* **99**:196–211. doi:10.1093/biolre/iy049
- 722 Soncin F, Morey R, Bui T, Requena DF, Cheung VC, Kallol S, Kittle R, Jackson MG, Farah O,  
723 Dumdie J, Meads M, Pizzo D, Horii M, Fisch KM, Parast MM. 2022. Derivation of  
724 functional trophoblast stem cells from primed human pluripotent stem cells. *Stem Cell*  
725 *Reports* **17**:1303–1317. doi:10.1016/j.stemcr.2022.04.013
- 726 Stranc LC, Evans JA, Hamerton JL. 1997. Chorionic villus sampling and amniocentesis for  
727 prenatal diagnosis. *Lancet* **349**:711–714. doi:10.1016/S0140-6736(96)08169-X
- 728 Sun T, Gonzalez TL, Deng N, DiPentino R, Clark EL, Lee B, Tang J, Wang Y, Stripp BR, Yao C,  
729 Tseng H-R, Karumanchi SA, Koeppl AF, Turner SD, Farber CR, Rich SS, Wang ET,  
730 Williams J, Pisarska MD. 2020. Sexually Dimorphic Crosstalk at the Maternal-Fetal  
731 Interface. *J Clin Endocrinol Metab* **105**:dgaa503. doi:10.1210/clinem/dgaa503
- 732 Takahashi S, Okae H, Kobayashi N, Kitamura A, Kumada K, Yaegashi N, Arima T. 2019. Loss of  
733 p57KIP2 expression confers resistance to contact inhibition in human androgenetic  
734 trophoblast stem cells. *Proc Natl Acad Sci U S A*. doi:10.1073/pnas.1916019116
- 735 Tanaka S, Kunath T, Hadjantonakis AK, Nagy A, Rossant J. 1998. Promotion of trophoblast stem  
736 cell proliferation by FGF4. *Science* **282**:2072–2075.
- 737 Varberg KM, Iqbal K, Muto M, Simon ME, Scott RL, Kozai K, Choudhury RH, Aplin JD, Biswell R,  
738 Gibson M, Okae H, Arima T, Vivian JL, Grundberg E, Soares MJ. 2021. ASCL2  
739 reciprocally controls key trophoblast lineage decisions during hemochorial placenta  
740 development. *Proc Natl Acad Sci U S A* **118**. doi:10.1073/pnas.2016517118
- 741 Viukov S, Shani T, Bayerl J, Aguilera-Castrejon A, Oldak B, Sheban D, Tarazi S, Stelzer Y,  
742 Hanna JH, Novershtern N. 2022. Human primed and naïve PSCs are both able to  
743 differentiate into trophoblast stem cells. *Stem Cell Reports* **S2213-6711(22)00457-X**.  
744 doi:10.1016/j.stemcr.2022.09.008
- 745 Wang BB, Rubin CH, Williams J. 1993. Mosaicism in chorionic villus sampling: an analysis of  
746 incidence and chromosomes involved in 2612 consecutive cases. *Prenat Diagn* **13**:179–  
747 190. doi:10.1002/pd.1970130305
- 748 Wang BT, Peng W, Cheng KT, Chiu SF, Ho W, Khan Y, Wittman M, Williams J. 1994. Chorionic  
749 villi sampling: laboratory experience with 4,000 consecutive cases. *Am J Med Genet*  
750 **53**:307–316. doi:10.1002/ajmg.1320530402
- 751 Wang L-J, Chen C-P, Lee Y-S, Ng P-S, Chang G-D, Pao Y-H, Lo H-F, Peng C-H, Cheong M-L,  
752 Chen H. 2022. Functional antagonism between  $\Delta Np63\alpha$  and GCM1 regulates human  
753 trophoblast stemness and differentiation. *Nat Commun* **13**:1626. doi:10.1038/s41467-  
754 022-29312-6
- 755 Wei Y, Wang T, Ma L, Zhang Y, Zhao Y, Lye K, Xiao L, Chen C, Wang Z, Ma Y, Zhou X, Sun F,  
756 Li W, Dunk C, Li S, Nagy A, Yu Y, Pan G, Lye SJ, Shan Y. 2021. Efficient derivation of  
757 human trophoblast stem cells from primed pluripotent stem cells. *Sci Adv* **7**:eabf4416.  
758 doi:10.1126/sciadv.abf4416
- 759 Williams J, Medearis AL, Bear MB, Kaback MM. 1987. Chorionic villus sampling is associated  
760 with normal fetal growth. *Am J Obstet Gynecol* **157**:708–712. doi:10.1016/s0002-  
761 9378(87)80034-0
- 762 Williams J, Wang BB, Rubin CH, Aiken-Hunting D. 1992. Chorionic villus sampling: experience  
763 with 3016 cases performed by a single operator. *Obstet Gynecol* **80**:1023–1029.
- 764 Yanagida A, Spindlow D, Nichols J, Dattani A, Smith A, Guo G. 2021. Naive stem cell blastocyst  
765 model captures human embryo lineage segregation. *Cell Stem Cell* **28**:1016-1022.e4.  
766 doi:10.1016/j.stem.2021.04.031
- 767 Yuen RKC, Robinson WP. 2011. Review: A high capacity of the human placenta for genetic and  
768 epigenetic variation: implications for assessing pregnancy outcome. *Placenta* **32 Suppl**  
769 **2**:S136-141. doi:10.1016/j.placenta.2011.01.003
- 770